

# Quantum tunneling of the magnetic moment

J. Tejada\*, J.M. Hernández, E. del Barco and X.X. Zhang

Departament de Física Fonamental, Universitat de Barcelona

## Abstract

In this paper we review the work done on magnetic relaxation during the last ten years on both single domain particles and magnetic molecules and its contribution to the discovery of quantum tunneling of the magnetic moment. We present first the theoretical expressions and their connection to quantum relaxation and secondly we show and discuss the experimental results.

Key words: Resonant spin tunneling, low temperature, magnetization, molecular clusters, single domain particles

## Resum

En aquest article presentem el treball realitzat en relaxació magnètica durant els darrers deu anys en partícules monodomini i en molècules magnètiques i la seva contribució al descobriment de l'efecte túnel del moment magnètic. En primer lloc, presentem les expressions teòriques i la seva connexió amb la relaxació quàntica, i, en segon lloc, mostrem i discutim els resultats experimentals.

Quantum objects have the property that their position always has some uncertainty. This is why, for example, helium liquid remains liquid even at absolute zero temperature: the quantum oscillations of the helium atoms are larger, even at zero temperature, than the interatomic distance. In other words, the quantum mechanical uncertainty in the position of helium atoms is greater than the distance between them, which makes their crystalline order at normal pressure impossible. Tunneling is the name given to the quantum mechanical penetration of potential barriers that in classical terms are insurmountable and is also a consequence of the uncertainty principle. Tunneling is, therefore, the explanation given when an electron confined within a certain volume literally disappears from inside that volume and reappears outside the volume. The tunneling microscope is an example of an application of such behavior.

One of the most interesting aspects of the behavior of nanomagnets is that their north and south magnetic poles may suddenly interchange due to quantum tunneling. Since magnetization is a classical vector, the phenomenon is also referred to as macroscopic quantum tunneling [1]. Such behavior may have important consequences in determining the lifetime of magnetic information storage when nanoscale magnets are used. For the magnetic moment of the nanometer particles will never block as a consequence of tunneling,

which, in turn, limits the storage density. However, the combination of mesoscopic particles and magnetic tunneling opens up the possibility of quantum computers. The memory unit of such a computer will be in a superposition of the spin-up (yes) and spin-down (not) states.

In this article we give an overview of our work over the last seven years on the search for the quantum tunneling of the magnetic moment. We present a brief review of: a) the physics underlying the dynamics of the magnetic moment of mesoscopic particles and domain walls, b) the use of low temperature relaxation measurements and c) the materials in which quantum tunneling of the magnetization vector (QTM) has been observed.

## The magnetic solid

The elementary carrier of magnetism in solids is the electron which has a magnetic moment of  $9.3 \times 10^{-21}$  e.m.u. Here e.m.u stands for the electromagnetic units. In magnetic solids such as iron and cobalt there is an interaction between the electrons which makes them point in the same direction. One cubic centimeter of these solids containing about  $10^{23}$  electrons has, therefore, a total magnetic moment of  $10^3$  e.m.u. The direction of this total magnetic moment is called easy axis of anisotropy and is determined by the magnetic anisotropy. The effect of the parallel alignment of electron magnetic moments is ferromagnetism, which disappears above what is known as the Curie temperature.

\* Author for correspondence: Javier Tejada, Departament de Física Fonamental, Universitat de Barcelona. Diagonal, 697. 08028 Barcelona, Catalonia (Spain). Tel. 34 93 402 11 58. Fax: 34 93 402 11 49. Email: jtejada@ffn.un.es.

We know, however, that magnetic solids below the Curie temperature may behave unlike magnets and become magnets after putting them in a strong magnetic field. This is because the magnetic ordering is not uniform at a macroscopic scale. There are magnetic domains inside which the magnetic moments of the electron are perfectly aligned and the magnetic moments of the different domains point in different directions. In zero field, the net effect may be zero and the body is not a magnet. When the solid is introduced into a strong magnetic field, the domains disappear and the ferromagnetic order is uniform in the solid. The magnetic domains appear immediately after the magnetic field is switched off and grow with time until reaching the final state of zero magnetization. If the material had a perfect atomic lattice with no defects or impurities, the net magnetic moment would become zero in a small fraction of a second. However, real solids have large concentration of defects which prevent domain walls from moving freely through the solid and permit permanent magnets to exist. This demagnetizing process due to domain wall diffusion inside the solids is called magnetic relaxation: in commercial permanent magnets at room temperature, it may take hundreds of years to reach zero magnetization state. At high temperature, however, the relaxation process may fully demagnetize a magnet in a few seconds. Our picture of thermal relaxation suggests, therefore, that the magnetic moment of a magnet will not relax at absolute zero temperature. At low temperature, however, relaxation continues due to quantum tunneling transitions which are independent of temperature [2, 3].

### Single-domain particles

A property of small ferromagnetic particles is that below a certain size they do not split into magnetic domains, i.e. such a particle is a uniformly magnetized single-domain. Mesoscopic particles of magnetic metals and oxides are single-domain; they are small magnets with a certain location of the north and south magnetic poles. In the absence of the external magnetic field, the energy of a single-domain particle does not change if its magnetic poles are interchanged. Consequently there is the same probability of finding the particle in either state. In the two states the energy of the particle is minimal. To take the magnetic poles of these two positions, that is to take out the magnetic moment from the easy direction, costs energy. This can be done by applying the external magnetic field at a certain angle to the easy axis direction. The magnetic poles return to their original positions after the external magnetic field is switched off.

Let us explain now in detail the time-dependent phenomena occurring in single-domain particles after the external magnetic field is changed. In the absence of the external magnetic field, the two equivalent but opposite orientations of the magnetic moment are separated by an energy barrier, on a linear scale with the volume of the particle (Fig. 1). The over-barrier transition probability at temperature  $T$  decreases exponentially with the ratio  $U/T$  where  $U$  is the barrier height and

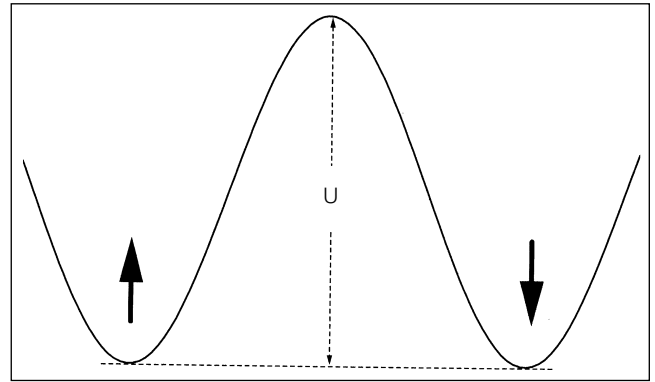


Figure 1.

$T$  is the temperature. If the thermal energy is greater than the barrier height, the magnetic moment oscillates rapidly between the two orientations, which corresponds to superparamagnetic behavior. As  $T$  is lowered, the magnetic moment becomes frozen in a particular direction. The temperature  $T$  at which the life time of a certain orientation is of the order of the experimental window time is called blocking temperature.

In 1988, it was predicted by Chudnovsky and Gunther [2] that at low temperature the magnetic moment could tunnel quantum-mechanically through the energy barrier with a probability  $\exp(-B)$  which is independent of temperature. One can define a crossover temperature  $T_C$  below which quantum under-barrier transitions dominate,  $k_B T_C = U/B$ .

For a collection of identical, non-interacting single-domain particles aligned in the same direction by a field, the anisotropy energy is universal throughout the system. As the magnetic field is switched off, the magnetization of the system relaxes as:

$$M(t) = M(t_0) \exp(-\Gamma t) \quad (1)$$

where  $\Gamma$  is the decay rate given by:

$$\Gamma = \Gamma_0 \exp(-U/k_B T_{\text{esc}}(T)) \quad (2)$$

Here  $T_{\text{esc}}(T)$  is what is called the escape temperature. For thermal transitions  $T_{\text{esc}}(T) = T$ , while for quantum under-barrier transitions,  $T_{\text{esc}}(T) = \text{cte}$ .  $\Gamma_0$  is the attempt frequency and is in the order of 1 GHz.

To observe the exponential relaxation in an array of single-domain particles, one needs a very narrow distribution of particle sizes, because  $\Gamma$  depends exponentially on the volume of the particle. While it is very difficult to prepare such a system, fortunately there are solids comprising identical molecular blocks in which it is possible to find an anisotropy barrier common to the entire system.

Real mesoscopic systems containing many volumes have, therefore, an exponentially large distribution of relaxation times. These systems always provide us with metastable states whose lifetimes can be examined using techniques like Mössbauer, ac and dc susceptibilities etc.. The disadvantage of these systems, however, is that only qualitative comparisons can be made with theory, due to the statistical nature of the processes. It is therefore very important to prepare systems with have one single barrier for all

metastable states with their lifetime time matching the experimental window time.

### Magnetic hysteresis and critical state

Suppose that a bulk ferromagnet has a hysteresis loop similar to the one shown in Fig. 2. If the field is changed from  $H_S$  to a field  $H_2$ , the magnetization will fall to a certain value,  $M_C$ , in a very short time, where a fine balance between the magnetic driving force and the pinning force on the domain walls is achieved. The magnetization  $M_C$  corresponds to the critical state. To reduce the total energy, the ferromagnet relaxes to its equilibrium state and assuming that it does not depart greatly from the critical state, the evolution of the barrier height with time can be written as [1]:

$$U = U_0 \left( 1 - \frac{M(t)}{M_C} \right) \quad (3)$$

This is equivalent to assuming that  $k_B T \ll U_0$ . The differential equation describing the relaxation process is:

$$\frac{dM(t)}{dt} = \Gamma M(t) \quad (4)$$

The integration of equation (4) gives:

$$M(t) = M(t_0) \left[ 1 - \frac{k_B T}{U_0} \ln(t/t_0) \right] \quad (5)$$

In the case of quantum depinning, we should replace  $T$  in equation (5) by a constant, in which case there is still relaxation but it is independent of temperature.

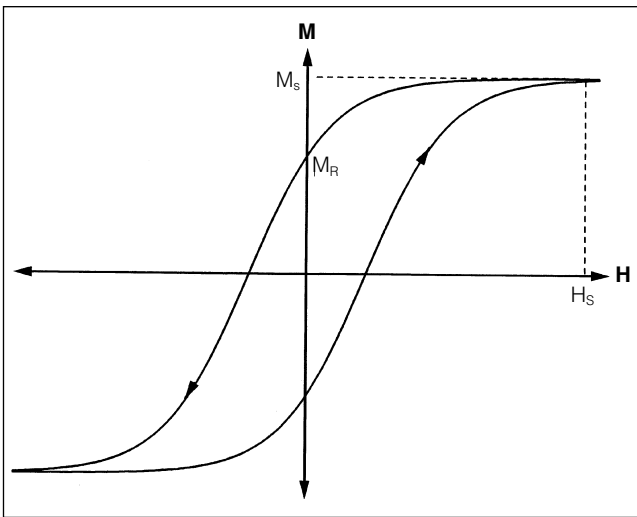


Figure 2.

### Energy barrier distribution

Most of the systems, such as bulk materials and systems composed of particles with different sizes and interaction between them, have a broad energy barrier distribution,  $f(U)$ . In this case, the time evolution of the magnetization after the field is removed is given by:

$$M(t) = M(t_0) \int_0^\infty f(U) \exp(-\Gamma t) dU \quad (6)$$

The blocking temperature can be defined as:

$$T_B = \frac{\langle U \rangle}{k_B \ln(\Gamma_0 t_{mes})}$$

where  $t_{mes}$  is the experimental measuring time, and  $\langle U \rangle$  is the average barrier height. At  $T \ll T_B$ , equation (6) can be approached [1] by:

$$M(t) = M_0 [1 - S(T) \ln(t/t_0)] \quad (7)$$

$$S(T) = \frac{k_B T}{\langle U \rangle}$$

In the vicinity of  $T_B$  the time interval in which the logarithmic law is valid is reduced and  $S(T)$  loses its linear dependence on  $T$ .

### Systems of particles with size distribution

Let us now investigate the case of non-interacting particles with a size distribution,  $f(V)$  [1]. Suppose that the easy axes of the particles are aligned in the same direction. After the field is removed, the time evolution of the magnetic moment is given by:

$$M(t) = M_0 \int_0^\infty V f(V) e^{-\Gamma t} dV \quad (8)$$

where,  $\Gamma = \Gamma_0 \exp(-KV/k_B T)$  is the transition rate of the magnetic moment between the two easy directions of a particle with volume  $V$  and anisotropy constant  $K$ ;  $M_0$  is the saturation magnetization of the particles, and  $N$  is the number of particles.

At a time  $t$ , only the particles with a volume  $V_R = k_B T \ln(\Gamma_0 t)$  contribute to relaxation, because smaller particles have already relaxed to their equilibrium state and bigger ones do not relax due to their small relaxation rate.

If, (Eq.8) is written as:

$$M(t) = N M_0 \left[ \langle V \rangle - \frac{1}{N} \int_0^{V_R(t)} V f(V) dV \right] \quad (9)$$

it is clear therefore that  $M(t)$  is a function of only  $V_R$ . Therefore, magnetic relaxation data obtained at different temperatures should scale in a  $M(t, T)$  vs.  $T \ln(\Gamma_0 t)$  plot, where  $\Gamma_0$  is a parameter fitting in the range of  $10^9 - 10^{12}$  Hz.

Since the typical experimental relaxation time is between  $10^{-10}$  to  $10^5$  s,  $V_R$  will change very little and (Eq.9) can be approached by:

$$M(t) = M(t_0) [1 - S(T) \ln(t)]$$

where the magnetic viscosity is given by:

$$S(T, t) = \frac{k_B T}{K \langle V \rangle} f(V_R) V_R \quad (10)$$

In Table 1, we summarize the temperature dependence of the magnetic viscosity obtained from Eq. (10) for several distributions [4].

Table 1. Temperature dependence of the viscosity for several distributions,  $f(V)$ .

$f(V)$	constant	$1/V$	$1/V^2$	log-normal
$S(T)$	$T^2$	$T$	constant	$\exp(-a \ln^2(T/T_B))$

## Magnetic clusters

The focus of chemistry is rapidly changing from the molecular to the supramolecular field, as the performance of sophisticated physico-chemical functions requires them to be correctly assembled in space so as to produce new large molecules with high spins and high anisotropy. This is also important in the new arena of molecular-based magnetism, in which «organic ferromagnetic» and «supramolecular» chemistry are paradigms.

The realization that the aims of both Chemistry and Physics are shifting to the supramolecular field is recent; as is the understanding that polynuclear compounds meet the requirements of low-temperature magnetic relaxation experiments. These systems are intermediate between purely paramagnetic molecules and mesoscopic systems. Therefore, the most remarkable differences between mesoscopic systems and high-spin polynuclear compounds relate to that a) the net spin of the polynuclear compounds is of quantum size while the spin for mesoscopic particles is measured in thousands, b) polynuclear compounds are composed of identical molecular building blocks and, consequently, there is a universal barrier height, whereas in real mesoscopic systems there is a distribution of barrier heights and c) the two wells associated with the anisotropy barrier contain, in the case of polynuclear compounds, a discrete spectrum of spin levels corresponding to the quantum orientations of the net spin of the system, while in mesoscopic particles there is a continuous distribution of energies for the different orientations of the total spin and the net magnetic moment.

## Experimental methodology

The key idea of magnetic relaxation is that, as one applies a magnetic field to a magnetic system, the magnetic moment of such a system has a two-step evolution. The first, the rapid step, finishes when the system reaches the critical state; and the second stage, the slow evolution, which is experimentally detected, occurs in the presence of barriers. We do not include in this category the magnetization delay due to eddy currents, which is an electromagnetic phenomenon, because high-frequency magnetic fields are not used in these experiments. We also do not consider the magnetization changes arising from structural modifications or aging of the system.

Suppose that the magnetic field acting on a physical system is suddenly changed from  $H_1$  to  $H_2$ . The magnetization

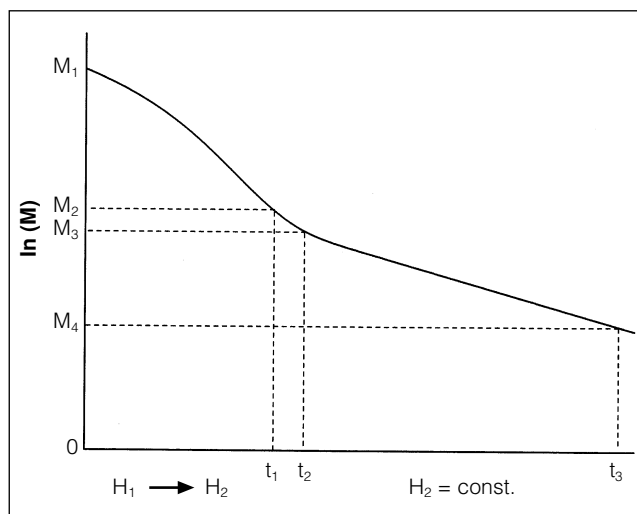


Figure 3.

of intensity  $M_1$  is immediately changed to a new value  $M_2$ . Then, after a certain waiting time whose value depends on the technique used, the variation of  $M_2$  with the time is recorded. This process is shown in Fig. 3. During the time  $(0, t_1)$  the magnetic field is changed,  $(t_1, t_2)$  corresponds to the waiting time before recording the variation of the magnetization and  $(t_2, t_3)$  is the time interval during which the variation with time of  $M_2$  is recorded.

The same interval  $(0, t_1)$  must always be used, so that the data can be compared, as is the case for example of the data recorded at different temperatures. It is so because the destruction of barriers depends on both the intensity of the magnetic field and the time during which it is acting. During the time interval  $(t_1, t_2)$ , the decay of the new value of the magnetic field should be zero. It is important to verify this point when using superconducting wires to generate the magnetic field. To avoid this decay, both fields,  $H_1$  and  $H_2$ , should be smaller than the first critical field of the superconductor that allows the improvement of the reproducibility of data. The best way to test this is to measure the magnetization of a calibrated paramagnetic sample as a function of time after changing the field to its new value  $H_2$ . The temperature should be constant throughout. It is also very important to achieve isothermal relaxation. In the fast relaxation process occurring between  $t_1$  and  $t_2$ , as well as in the slow process from the critical state, there is a release of magnetic energy which can cause local heating. Therefore, we have to take into account the power  $P = -dE/dt$ , where  $E$  is the total energy of the system and  $P$  is the power of the total losses taking place. Therefore, we should distinguish the energy losses occurring before the critical state is reached, from those associated with the slow relaxation of the system, when the magnetic field is constant.

Let us quantify the self heating in a real experiment [4,5], corresponding to the relaxation of a very thin film of composition  $\text{Fe}_3\text{Tb}$  with a mass  $m = 1.92 \times 10^{-4}$  g at the temperature  $T = 1.7$  K. Initially, when the field is  $H_1 = 100$  Oe. the magnetization is  $M_1 = 3.745 \times 10^{-3}$  emu. After changing the magnetic field to its new value  $H_2 = -100$  Oe. the magnetization is

$M_2 = 1.7887 \times 10^{-3}$  emu. That is, the energy variation is  $\Delta E = 5.5 \times 10^{-1}$  erg, and the corresponding temperature change may be evaluated using the expression  $\Delta T = \Delta E/m$  where  $m$  is the specific heat of the system,  $= 7 \times 10^{-4}$  erg/gK. This gives  $\Delta T = 10^{-2}$  to  $10^{-3}$  K. In the slow relaxation process, the energy variation is one order of magnitude smaller and consequently the temperature change is negligible. In conclusion it seems clear that the self-heating phenomenon in the relaxation experiments carried out in the kelvin regime does not play any important role. The situation, however, can be different when the temperature of the system is in mK range. Though the magnetic energy release is of the same order or smaller than above, neither the variation in temperature nor the time needed to reach thermal equilibrium can not be fully ignored.

### Theoretical considerations

The crossover temperature from classical to quantum regime [1,2,6] is:

$$T_C \approx (\mu_B / k_B)(H_{//}/H_{\perp})^{1/2} \quad (11)$$

where  $H_{//}$  is the easy anisotropy field and  $H_{\perp}$  is the field responsible for the non-commutation of the magnetization vector  $M_{//}$  with the Hamiltonian.  $T_C$  is, therefore, characteristic for each material and does not depend on extensive parameters like the volume of the particle. The fact that  $T_C$  scales with the magnetic anisotropy constant  $K$  of the material ( $K = 1/2 H_{//} M_S$ ) (where  $M_S$  is the saturation magnetization), may be easily verified using particles with different anisotropy. When considering the tunneling volume, it is important to notice that the pre-exponential factor  $\Gamma_0$ , entering in the relaxation rate given in equation (2) is of the order of  $10^{10} \text{ s}^{-1}$ . Thus, if one wants to observe quantum relaxation processes that take hours, the tunneling exponent  $B$  ( $\Gamma = \Gamma_0 \exp(-B)$ ) should not exceed 25. This limits the volume of the magnetic particle,  $V = 25 k_B T_C / K$ . The size of the particles showing tunneling and the temperature at which this tunneling takes place depend on the value of the external magnetic field because of the modification of the barrier heights with the field.

For nanoscale antiferromagnetic particles which have small non-compensated magnetic moments due to finite size effects, the expression to calculate the crossover temperature is [1,7]:

$$T_C = \frac{\mu_B}{k_B} \left( \frac{K_{//}}{\chi_{\perp}} \right) \quad (12)$$

where  $K_{//}$  is the anisotropy constant and  $\chi_{\perp}$  is the magnetic susceptibility. The tunneling exponent  $B = 25$  can be matched by particles which are bigger than the ones in ferromagnetic tunneling. Materials for which the value of  $K_{//}$  is of the order of  $10^6$  erg/cm<sup>3</sup> and have  $\chi_{\perp} = 10^{-4}$  should exhibit quantum effects above a few kelvin [8].

## Experiments on quantum magnetic relaxation

### Nanoscale CoFe<sub>2</sub>O<sub>4</sub> particles dispersed in water.

Co Fe<sub>2</sub>O<sub>4</sub> is an inverse spinel with very large magnetic anisotropy,  $K = 10^7$  erg/cm<sup>3</sup>. Therefore, a system formed by mesoscopic particles of this spinel should constitute a well-defined arena in which to observe quantum tunneling processes at temperatures of a few kelvin. In Fig. 4, we show the hysteresis loop obtained at 2.4 K. In this figure, one feature that should be noted is the non-closed loop up to 5 T (see the inset), which indicates that the anisotropy field is not smaller than 5 T. By substituting the value of the anisotropy field,  $H_K = 5$  T, of these particles into the theoretical expression giving the crossover temperature, we find that  $T_C = 5$  K. The average diameter of the particles we prepared is 60 Å. In Fig. 5, we show the ZFC and FC curves obtained under different applied fields. As expected, as the field increases, the blocking temperature shifts to lower temperatures due to the reduction in the barrier heights. The relaxation was measured by cooling the sample from room temperature in a field  $H_1 = 0.5$  T and, after arrival at the target temperature, applying a new field  $H_2 = -0.4$  T.

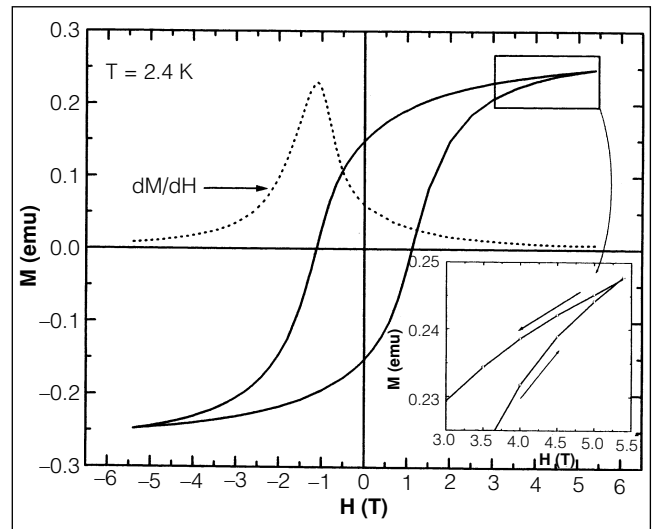


Figure 4.

In Fig. 6, we show the magnetization vs time on a logarithmic scale. The extracted values of the magnetic viscosity are shown in Fig. 7. From this figure, it is clear that between 5 and 2.5 K the viscosity changes in line with the temperature. These values are extrapolated to zero for  $T = 0$  K, which indicates that the interaction between particles is much smaller than the energy barrier height. This is clear, in this case, because the effective dipole field due to the interaction between particles is much less than 0.01 T and because we are dealing with anisotropy barriers corresponding to a field of 5 T. Below 2.5 K, we observe a plateau in the viscosity and that the  $M(t)$  data do not keep to scale any more on the  $\ln(t)$  plot (Fig. 8) [9, 10].

The above two experimental observations point toward the occurrence of non-thermal relaxation processes, which is

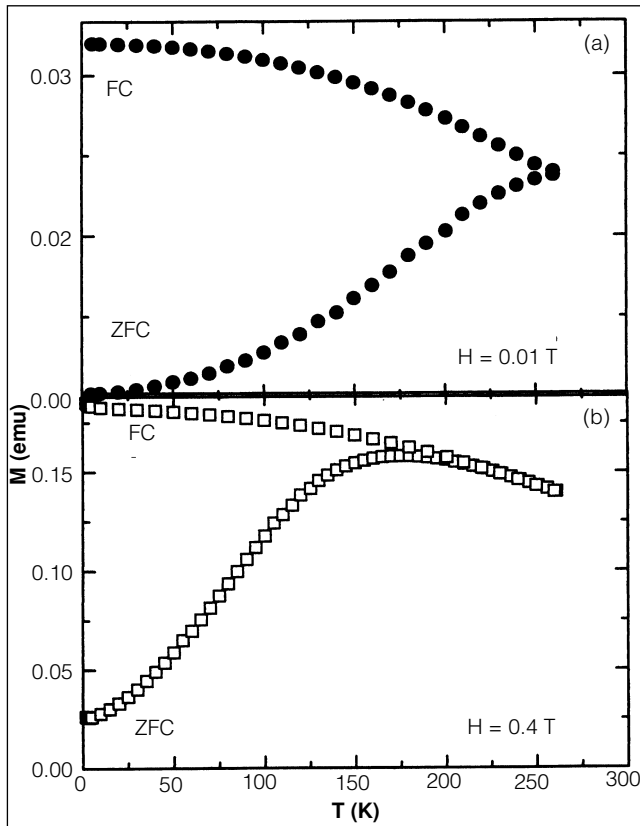


Figure 5.

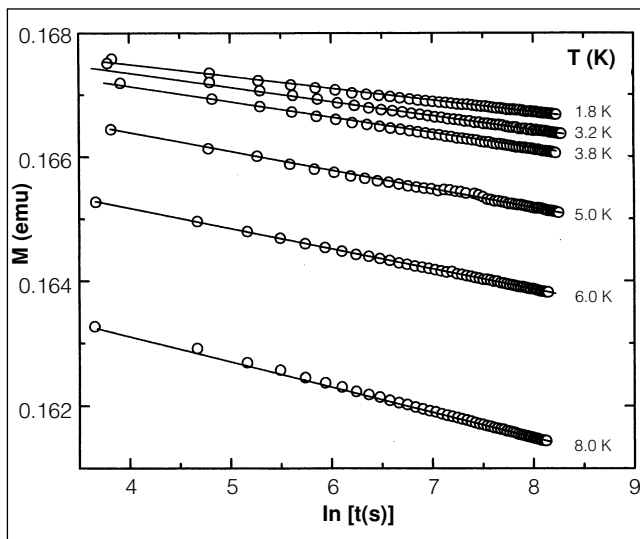


Figure 6.

consistent with that, for this high anisotropy material, low-temperature relaxation is dominated by quantum tunneling out of metastable states rather than by thermal transitions. The experimental crossover temperature of 2.5 K is consistent with the temperature suggested by theory, 5 K. Very similar results have been obtained in other mesoscopic particles or grains owing to their high magnetic anisotropy [11-14].

**Mesoscopic granular materials**

The atomic evaporation of rare earth and other metals by using electron beam evaporation technique enables very thin films to be prepared. These structures are useful in the

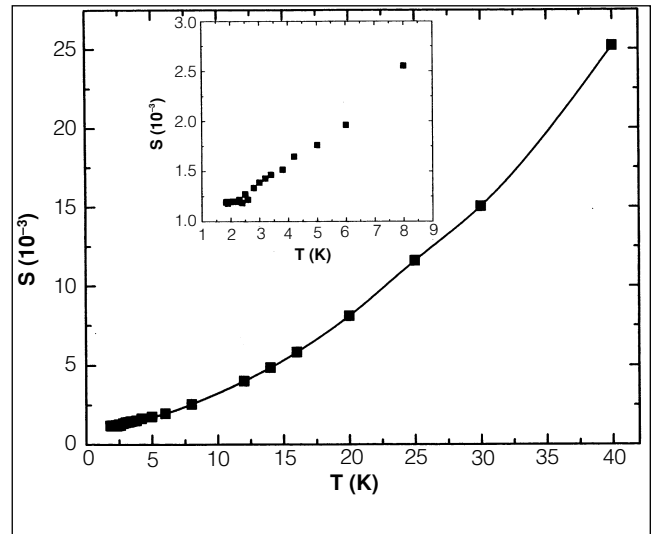


Figure 7.

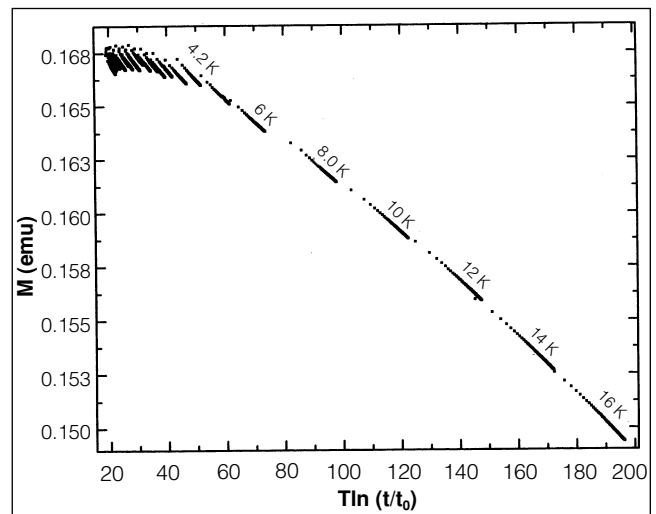


Figure 8.

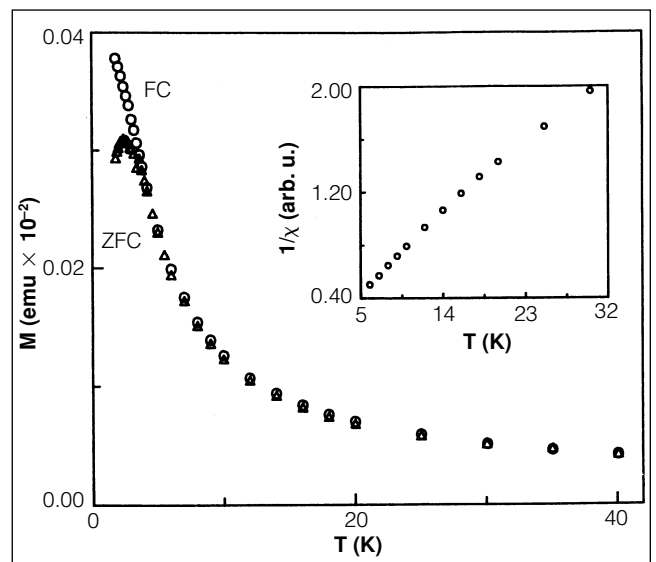


Figure 9.

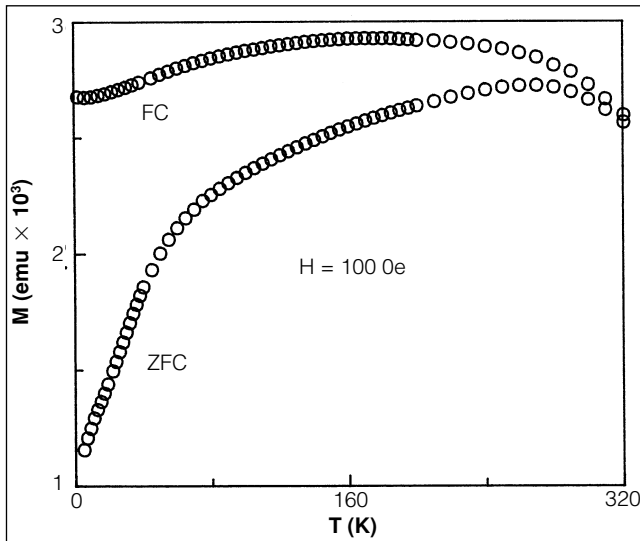


Figure 10.

study of quantum tunneling of magnetization. For example, the evaporation of Dy and Cu produces samples with mesoscopic grains of Dy imbedded in a Cu matrix; or on simultaneous evaporation of Tb and Fe, samples with magnetic clusters of nanometer size are produced. The atomic magnetic moments in these systems are ferromagnetic correlated on a small scale ( 100 Å ), while on a large scale the magnetization vectors rotate stochastically over the whole sample. In this section, we show results obtained for two samples, one a Dy/Cu multilayer of composition  $[\text{Cu}(100 \text{ \AA}) / \text{Dy}(40 \text{ \AA})]_{x20}$  and the other one a random magnetic film comprising many  $\text{Fe}_3\text{Tb}$  clusters of few nanometer in size.

In these materials, the existence of ferromagnetic clusters, as well as their size distribution, may be univocally verified by measuring the ZFC and FC magnetization. The detection of a blocking temperature, which is shifted with the field intensity, and the irreversibility between the ZFC and FC curves below the blocking, are clear indications of the existence of magnetic clusters. In Figs. 9 and 10 we show the ZFC and FC curves for the Dy multilayer and the Tb random magnet. From the blocking temperature we estimated the average energy barrier,  $30K_B T_B = U = KV$ , of both the Dy and  $\text{Fe}_3\text{Tb}$  clusters existing in the samples. Taking the value for K that has been experimentally determined from the isothermal  $M(H)$  high-field measurements, we got the average activated magnetic volume for each sample, which is about  $V = 2000 \text{ \AA}^3$  for the two. The ZFC and FC data for both samples were extended to the lowest temperature of 1.7 K.

These systems show long-term magnetic relaxation down to 1.7 K, which obeys very well logarithmic law. From these data and using the criterion of the critical state we calculated the magnetic viscosity,  $S(T) = dM/d\ln(t)$  [1, 3, 15]. In Figs. 11 and 12 we show the variation of viscosity with temperature for both samples. In the case of the sample containing the  $\text{Fe}_3\text{Tb}$  clusters we performed experiments using different applied fields as well.

Different features can be observed from Figures 11 and 12:

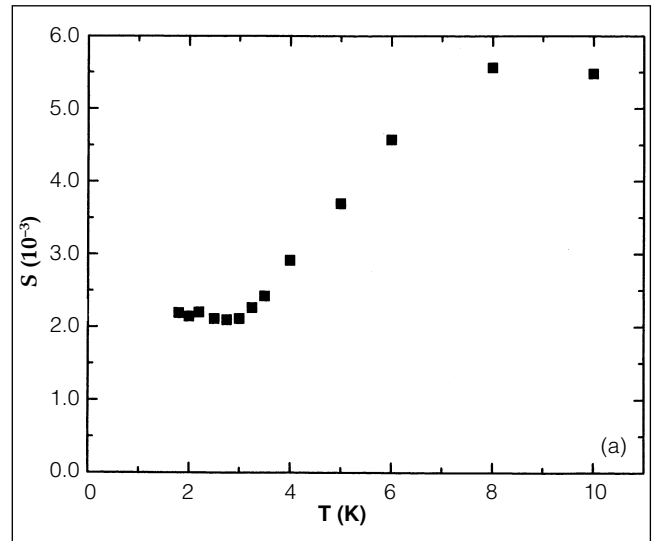


Figure 11.

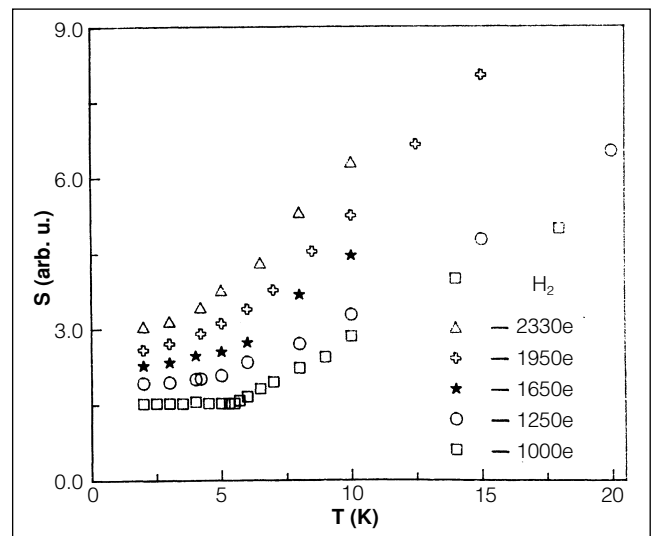


Figure 12.

- $S(T)$  has a maximum at temperature  $T < T_B$ .
- $S(T)$  decreases when the temperature from  $T_B$  decreases until it reaches the lowest temperature interval at which  $S$  is constant.
- The temperature,  $T_C$ , below which  $S$  is constant depends on the anisotropy field of the sample.
- The values of both  $S(T)$  and  $T_C$  depend on the magnitude of the magnetic field applied during the relaxation.

All these data, together with those of the magnetization vs temperature which are consistent with the existence of a regular and broad distribution of energy barriers, suggest, as the most plausible interpretation, the occurrence of quantum tunneling of the magnetization vector at low temperature.

#### Antiferromagnetic particles of horse-spleen ferritin

Ferritin is a very large clathrate compound consisting of a protein cage for an «iron core» of the mineral ferrihydrite combined with a phosphate [16]. The space allowed for the mineral is a sphere of about 80 Å in diameter and is able to

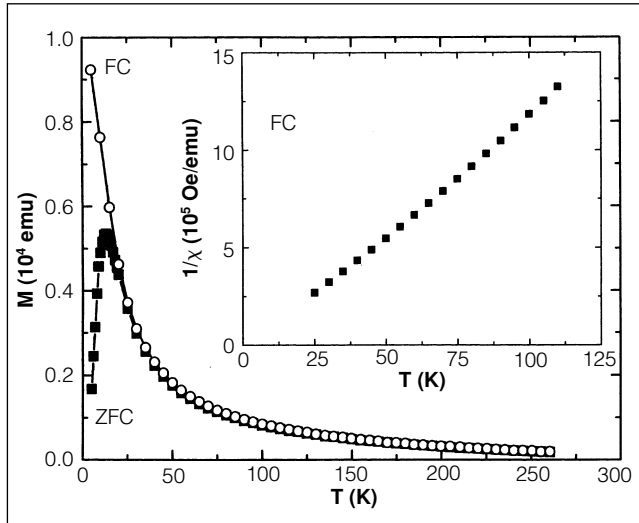


Figure 13.

store up to  $4500 \text{ Fe}^{3+}$ . In our experiments we used a sample containing  $1.2 \times 10^{16}$  protein molecules. The magnetization detected in this sample is due to the spin non-compensation in the two ferromagnetic sublattices which are antiferromagnetically coupled. The value of the spin non-compensation was deduced from the low temperature variation of the magnetization above the blocking which occurs at 13 K [17, 18], see Fig. 13. Our estimate is that the average number of non-compensated surface spins per molecule is 15. The relaxation follows the  $\ln(t)$  law as expected due to the broad distribution of particles of different size and in line with the data of the low-field magnetization in the ZFC and FC processes. The magnetic viscosity data were calculated in the framework discussed above for a system of independent particles which are distributed in size, the barrier height for the magnetic moment being proportional to the volume. The plateau observed below 2.1 K (see Fig. 14) indicates that this is the value of the crossover temperature from classical to quantum behavior. This corroborates the theoretical prediction of  $T_C$  that gives 3 K. We also calculated the tunneling volume from its relation with the WKB exponent  $B = (V/\mu_B) (\chi_{\perp} H_{\parallel})$ . We

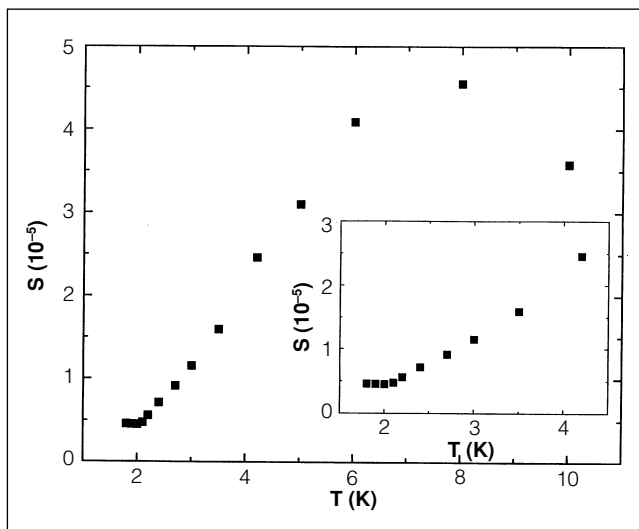


Figure 14.

found that  $V = 8 \times 10^4 \text{ \AA}^3$  corresponding to particles with diameter smaller than  $50 \text{ \AA}$ . In conclusion, these data show that at high temperature both the Néel vector  $\mathbf{L}$  and the net magnetization vector are jumping above the barriers between  $\mathbf{L}$  and  $-\mathbf{L}$  states, while below 2.1 K the change in the direction of the two vectors is due to the tunneling effect [1, 17].

#### FeTbO<sub>3</sub> Orthoferrite single crystal.

FeTbO<sub>3</sub> crystallised in an orthorhombic distorted perovskite structure which belongs to the space group Pbnm. In this section we will only discuss the low temperature data, more precisely for  $T < 3.1 \text{ K}$  where the  $\text{Fe}^{3+}$  spin configuration is that of a canted antiferromagnet and the  $\text{Tb}^{3+}$  spins order cooperatively.

The exponential decay of the remanent magnetization in the TbFeO<sub>3</sub> [19] orthoferrite single crystal suggests that this system has a single barrier;  $\Gamma$  is therefore the inverse of the lifetime of the metastable magnetic state and is valid for the whole system. The decay rate  $\Gamma$  can be expressed in terms of the escape temperature  $T^*$  defined by the relation:

$$\Gamma = \omega \exp\left[-\frac{U(H)}{k_B T^*(T)}\right], \quad (13)$$

where  $U(H)$  is the energy barrier which depends on the applied field. Therefore:

$$\ln \Gamma = C - \frac{U(H)}{k_B T} \quad (14)$$

where  $C = \ln(\omega)$ . The plot of  $\ln \Gamma(T)$  versus  $1/T$  shows that the Boltzmann activation regime occurs at temperatures higher than 2.3 K (Fig. 15). Thus the values of  $C$  and  $U(H)/k_B$  are obtained from the linear fit of  $\ln \Gamma$  versus  $1/T$ . Then the values of  $C$  and  $U(H)/k_B$  were used to determine  $T^*(T)$  throughout the temperature range  $1.8 \text{ K} \leq T \leq 3.1 \text{ K}$ , from the following relation:

$$T^*(T) = \frac{U(H)}{k_B} [C - \ln \Gamma(T)]. \quad (15)$$

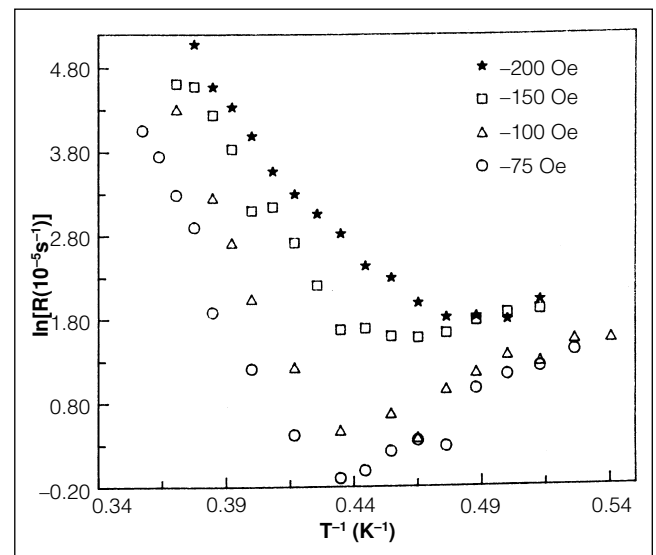


Figure 15.



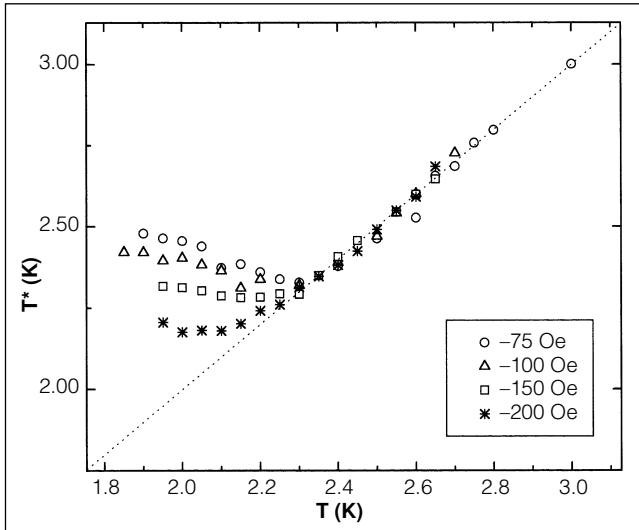


Figure 16.

The values of  $T^*(T)$  obtained are shown in Fig. 16.

From the above results, the following features are observed:

1. The escape rate has two clear regimes: at  $T \leq 2.3$  K,  $\Gamma(T)$  changes exponentially with temperature, while it remains near constant at lower temperatures.

2. The values of escape temperature  $T^*(T)$  are the same as  $T$  at high temperatures and greater than  $T$  at temperatures lower than 2.1 K for  $H_2 = -200$  Oe.

The fact that  $T^*(T)$  is exactly equal to  $T$  above the crossover temperature,  $T_C$ , is in accordance with the theoretical expectation of Boltzmann activation in the classical regime. Moreover, the extrapolation of this curve to  $T = 0$  K gives  $\Gamma(0) = 0$ , indicating that at  $T = 0$  K the thermal relaxation processes would be frozen out. The existence of a near plateau in the  $T^*(T)$  dependence at low temperature is exactly what is to be expected in the presence of quantum depinning of domain walls. The fact that  $T^*$  is not exactly constant below the crossover temperature may be related to the variation with temperature of the order parameter characterizing the reorientation transition of the  $\text{Fe}^{3+}$  spin system below 3.1 K. It has been suggested that the crossover temperature for domain wall tunneling may be of the same order of magnitude for antiferromagnets as for small antiferromagnetic particles [19]:

$$T_C = \frac{\mu_B}{k_B} \sqrt{\frac{K}{\chi}}, \quad (16)$$

where  $K$  is the anisotropy constant,  $K = 1.15 \times 10^5$  erg/cm<sup>3</sup>, and  $\chi$  is the initial susceptibility,  $\chi = 10^{-4}$  [20]. We have that the theoretical prediction is  $T_C \sim 2.2$  K, in accord with our experimental value of  $T_C \sim 2.1$  K.

It is clear that the relaxation process in this material is determined by the dynamics of antiferromagnetic domain walls. The nature of the single energy barrier for the displacement of a domain wall below 3.1 K is not clear. However, one possibility is thermal or quantum escape from a universal pinning center. The question remains as to what

explanation can be provided for the universal pinning center and consequently the existence of a single barrier height throughout the whole single crystal. Here two possibilities are discussed for such behavior. It is well known that the dynamic of domain walls is governed by the pinning centers created by impurities, defects and grain boundaries. In ceramic single crystals only the impurities entering the lattice during the growth process are responsible, in most cases, for the pinning centers. In the  $\text{TbFeO}_3$  single crystal there are lead impurities detected spectroscopically [21,22]. However, the barrier due to these impurities is too small to explain the barrier in the relaxation measurements. Yet, if pinning is due to the cluster of impurity, it is hard to explain a single barrier height. The second possibility refers to the fact that Tb may have domain walls which separate domains with the same orientation of Tb moments and differ only in the orientation of the Néel Vector. This is possible because the  $\text{Fe}^{3+}$  lattice and the  $\text{Tb}^{3+}$  lattice belong to different representations of the symmetry group of the crystal. Therefore, there should be planar Tb domain walls in the crystal, which interact very weakly with the magnetic field but can pin Fe domain walls. This would provide pinning of Fe walls by planar defects, very similar to the one described in [23].

#### Experiments on quantum hysteresis and resonant spin tunneling

The case of interest now is when all the particles have the same size and shape. However, this cannot be achieved with mesoscopic particles. But identical molecular clusters with the two ingredients for studying magnetic relaxation, i.e. spin and magnetic anisotropy, do exist. In this case, there is a universal barrier height for the magnetic moments of the particles and the only problem is practical: the relaxation time must match the experimental window time. Clearly this will greatly reduce the possibility of performing experiments, but hopefully chemists will rapidly improve their way of preparing molecular clusters by controlling, essentially, the mag-

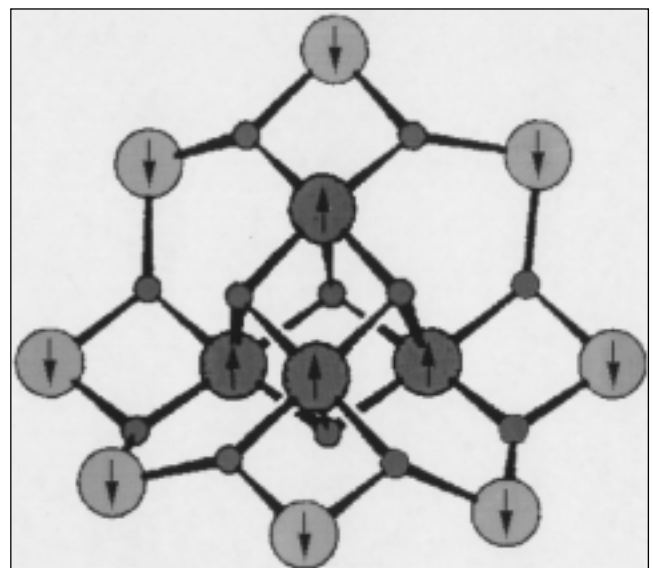


Figure 17.

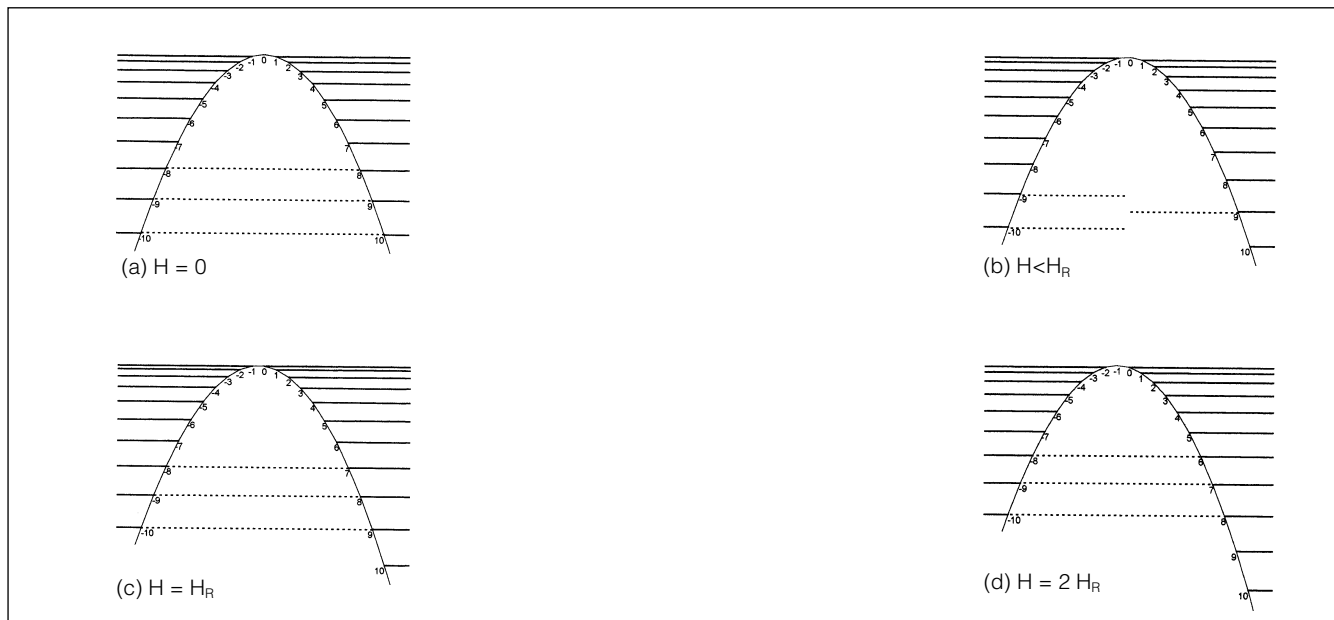


Figure 18.

netic anisotropy. This is not, however, a simple question because the value of the magnetic anisotropy constant affects exponentially the relaxation time and in consequence small variations in that constant may produce dramatic changes in the relaxation time.

We now discuss some of the recent results obtained for these materials and explain the physics underlying the phenomena [24,28]. The material studied is a molecular crystal of unit formula  $\text{Mn}_{12}\text{O}_{12}(\text{CH}_3\text{COO})_{16}(\text{H}_2\text{O})_4$ . In the crystal the molecules exist in a tetragonal lattice. The unit cell contains two  $\text{Mn}_{12}\text{O}_{12}$  molecules surrounded by four water molecules and two acetic acids. The structure of the  $\text{Mn}_{12}\text{O}_{12}$  molecule is shown in Fig. 17. It has a tetrahedral core of four  $\text{Mn}^{4+}$  ions in its center, surrounded by the crown of eight  $\text{Mn}^{3+}$  ions. Each of the  $\text{Mn}^{3+}$  ions has spin  $3/2$ , while each of the  $\text{Mn}^{4+}$  ions has spin 2. The total net spin of the molecule is, therefore,  $S=10$ . Due to the acetate shell, each molecule is well isolated from the others. The symmetry of the lattice molecule gives strong uniaxial anisotropy along the  $c$ -axis. In the absence of the external magnetic field the two possible orientations of the total spin  $S=10$  are separated by an energy barrier  $U = 60 \text{ K}$  ( $U = 5 \times 10^{-4} \text{ eV}$ ). Fig. 18. It has been well established from dc-magnetic measurements using low magnetic fields that the temperature at which the magnetic moment, or spin, jumps the barrier with the frequency of 0.1 Hz is about 3 K. Below this temperature there are hysteresis phenomena due to the existence of metastable states associated with the 21 different orientations of the total spin  $S=10$ .

When an external magnetic field is applied, one of the two wells becomes metastable. It is suggested that the energy of the different spin levels in this system is described by the Hamiltonian:

$$H = -DS_z^2 + g\beta SH \quad (17)$$

where  $D$  is the anisotropy energy constant and  $H$  is the applied magnetic field. The solution of this Hamiltonian on the basis of a set of the 21 states  $|S, S_z\rangle$  with  $S = 10$ , shows that there are certain values for the magnetic field, called crossing fields, in which the spin levels in the two wells have the same energy ( see Fig. 19 ). In fact, this occurs at constant intervals in the magnetic field.

The results presented here were obtained from a sample in which the  $c$ -axes of the molecules were oriented in the same direction by an external field [5,28][AE1]]. In Fig. 20, we show  $M(H)$  data, obtained at different temperatures, after zero-field cooling of the sample to the measuring temperatures. The jumps in the hysteresis loops appear at constant intervals of the applied magnetic field. The existence of the jumps is well understood in the contrast of the above Hamiltonian. As the external applied field increases from zero, the degeneration of the two wells is broken and magnetization grows as a consequence of the alignment of the magnetic

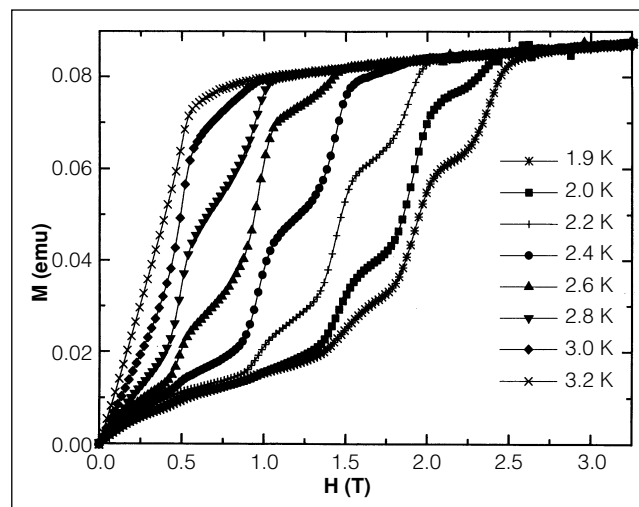


Figure 19.

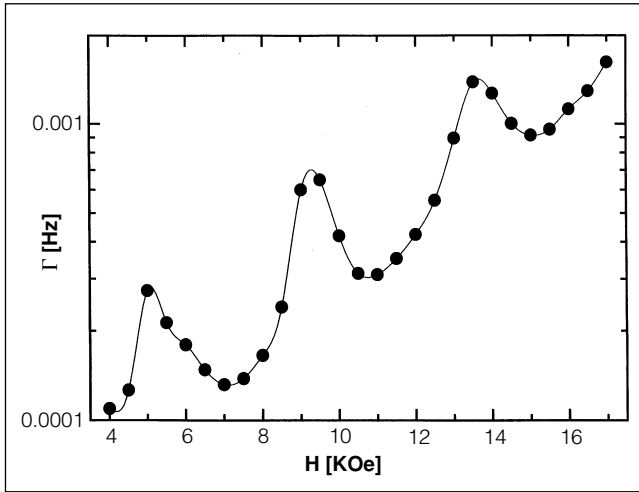


Figure 20.

moments of the molecules along the magnetic field. When the applied field reaches the value of the first crossing field, the resonant tunneling processes occur between the levels of the two wells which have the same energy. Consequently, the tunneling leads to a faster variation of the magnetization. When the external applied field is further increased, the system reaches the next crossing field and new jumps appear.

We also studied the variation of the relaxation rate with the field at different temperatures [26,27]. The sample is first zero-field cooled, then the field is applied, and the variation of magnetization with time is detected over two hours. The relaxation of the magnetization follows quite well the exponential law from which the relaxation rate was extracted (Fig. 21). From this figure, it is clear that the jumps in the relaxation rate appear at the same fields as the jumps in the hysteresis loops. Moreover, as the temperature rises, the height of the jumps in the relaxation rate increases. This could be interpreted in terms of the occurrence of a thermally assisted resonant tunneling process. When the temperature increases, the levels near the top of the metastable wells are more populated, and, consequently, the relaxation rate increases.

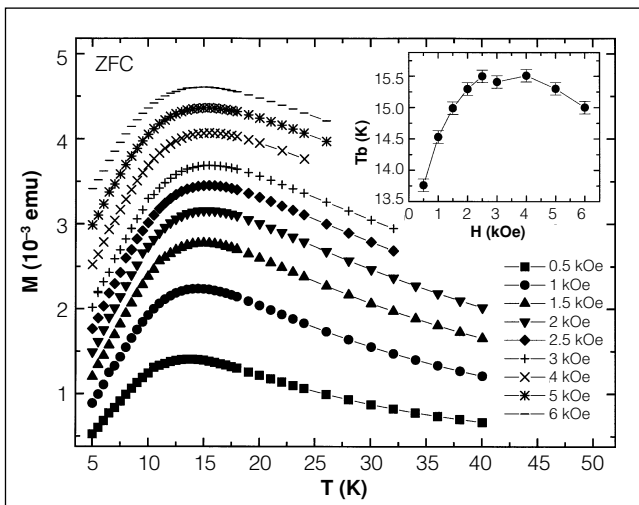


Figure 21.

### Experiments on macroscopic resonant tunneling

In this section we will describe the experiments carried out in order to elucidate the occurrence of resonant tunneling at macroscopic level [29].

Just after observing the resonant spin tunneling for quantum spins of value 10, we started thinking about a similar observation of a macroscopic particle. The ideal system should be identical macroscopic particles with very high anisotropy and with a relatively small magnetic moment, i.e. we would have well-defined spin levels in the two wells of the anisotropy. Ferromagnetic particles are not good because of the high value of their total spin but antiferromagnetic particles with non-compensation spin are a better choice. The question of the distribution of sizes remained unsolved and consequently we should think in a experimental itinerary in which the distribution of the size of particles were more an advantage than an inconvenience. The solution came with the idea of magnetic relaxation.

From the classical point of view, the magnetic field applied to a magnetic particle lowers the barrier between the directions of the moment along and against the field. Consequently, one should expect  $T_B$  to decrease as the field increases. This is, in fact, common behavior in systems of small particles. However, in ferritin the dependence of  $T_B$  on  $H$  is different. As is shown in the inset to Fig. 22, the blocking temperature has a nonmonotonic dependence on the field.. Additional evidence for this behavior comes from measurement of the ac susceptibility. In these measurements, as compared to the dc-ZFC magnetization measurements, the role of time is played by the frequency of the ac-field.

Correspondingly, the blocking temperature is determined by:

$$T_B = \frac{U}{\ln(1/f\tau_0)} \quad (18)$$

The higher the frequency, the larger the  $T_B$ . This allows one to conduct an independent test of whether the moments of the particles are frozen at low temperature by their individ-

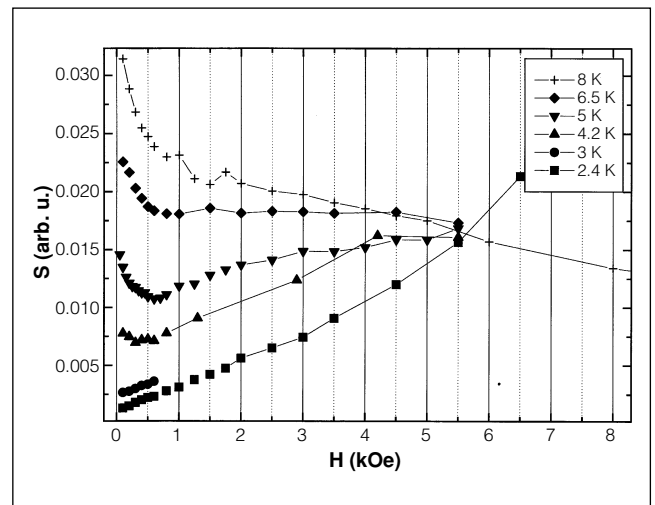


Figure 22.

ual anisotropy barriers or by interactions. The ac measurements show that  $T_B$  in natural ferritin does depend on frequency in accordance with equation (18), providing an independent proof for the single-particle nature of the effect. This conclusion is also supported by Mössbauer measurements for frequencies as high as  $f \sim 4 \times 10^8$  Hz.

The following procedure was used to measure relaxation. The ferritin sample was cooled in zero field from 50 K down to the measurement temperature. The magnetic field was then applied and the sample was allowed to relax to the equilibrium state. With high accuracy the relaxation is logarithmic in time for four decades, as it should be in a system with broad distribution of energy barriers. The quantitative measurement of relaxation is the magnetic viscosity defined as:

$$S = \frac{1}{M_{\text{eq}}(H, T)} \frac{dM(H, T, t)}{d \ln(t)}, \quad (19)$$

where  $M_{\text{eq}}(H, T)$  is the equilibrium magnetization of the system at fixed temperature and field. The latter was deduced from the field-cooled magnetization measurements.

As has been previously reported [17], at a small field ( $H \sim 100$  Oe) viscosity is independent of temperature below 2.4 K, which points to the quantum origin of low-temperature magnetic relaxation in ferritin. This is in accordance with the temperature of the crossover from thermal to quantum regime, predicted by the theory [3,6,7].

Viscosity as a function of the applied field at different temperatures is plotted in Fig. 23. At  $T = 2.4$  K and  $T = 3$  K it increases monotonically with the field. Between 3 and 8 K the viscosity first drops as the field increases from zero, then reaches minimum at a certain field that depends on temperature, and then increases at greater fields. Above 8 K the viscosity monotonically decreases with the field. This is our main experimental finding and confirms the conclusion drawn from the field dependence of  $T_B$  and  $dM/dH$ : in a certain temperature range the system relaxes faster in zero field than it does at a non-zero field.

This unusual behavior of the magnetic relaxation in ferritin can be explained if one takes into account quantization of spin levels in ferritin molecules. The low-lying levels must be separated by the energy of the antiferromagnetic resonance,  $\epsilon = (2\epsilon_{\text{an}}\epsilon_{\text{ex}})^{1/2}$ , which is huge compared to the separation of spin levels in a ferromagnetic particle of a comparable size. In ferritin this separation must be of order of the 10 K, i.e. comparable to the separation of low lying levels in Mn-12 molecules of spin 10. This suggests that *the resonant spin tunneling recently observed in Mn-12 molecules [25-28] can also be observed at macroscopic level in ferritin molecules containing a few thousand iron atoms*. The argument goes as follows: Consider an individual ferritin molecule in the magnetic field  $\mathbf{H}$  opposite to its total spin  $\mathbf{s}$ . This is a metastable state tending to decay towards the direction of the field. The resonant tunneling between the spin levels occurs when  $2g\mu_B Hs = n\epsilon$ , where  $n = 0, 1, 2, \dots$ , that is, at values of the magnetic field separated by:

$$\Delta H = \frac{H_{\text{an}}}{2S} \left( \frac{2\epsilon_{\text{ex}}}{\epsilon_{\text{an}}} \right)^{1/2} \quad (20)$$

For a ferromagnetic particle of spin  $S$ , the field separation between resonances is  $H_{\text{an}} / 2S$  [30], which for  $H_{\text{an}} \sim 1$  kOe and  $S \sim 10^4$  gives  $\Delta H \sim 0.1$  kOe. This would certainly be smaller than the width of the levels (the ferromagnetic resonance width) and, thus, unobservable. For an antiferromagnetic particle, however, due to the smallness of the non-compensated spin and the exchange enhancement of the anisotropy, the field spacing of resonances is greater by a factor  $(S/s) (\epsilon_{\text{ex}}/\epsilon_{\text{an}})^{1/2}$ , which is of the order of  $10^4$  in ferritin. Consequently, the field spacing between resonances in ferritin must be of the order of kOe, e.i. comparable to that in Mn-12. However, due to the different orientation and magnitude of the non-compensated spin, different from a Mn-12 crystal, only the  $H = 0$  resonance occurs simultaneously in all ferritin molecules.

As in Mn-12, tunneling between different spin orientations in ferritin in our temperature range must be thermally assisted; that is, it occurs from excited spin states as well as from the ground state. The spin states are characterized by the projection of  $\mathbf{s}$  on the anisotropy axis,  $s_z |m\rangle = m|m\rangle$ . At  $H = 0$  the states corresponding to  $m$  and  $-m$  have exactly the same energy and the resonant tunneling between these states takes place. At low temperature (below 3 K) only the lowest levels  $m = \pm s$  are occupied. The tunneling splitting of these levels is extremely small, about  $10^{-4}$  Oe. This should explain why we do not see the  $H = 0$  peak in the viscosity at low temperature. As the temperature increases above 3 K, higher  $m$  levels become thermally populated and tunneling between them dominates relaxation. These levels must be wide due to their finite lifetime with respect to the decay down to the ground state levels  $m = \pm s$ . Consequently, the width of the resonance on the magnetic field becomes large enough to observe the  $H = 0$  maximum in the magnetic viscosity. As the temperature continues to increase towards the blocking temperature, the system enters the superparamagnetic regime and viscosity monotonically decreases with the field, reflecting the progressive disappearance of metastability.

## Conclusions and remarks

In conclusion, we have shown that magnetic relaxation studies of nanostructured materials enable quantum tunneling processes of the magnetization vector to be observed. In the case of single-domain particles and magnetic clusters with broad size distribution, the relaxation law is logarithmic and the magnetic viscosity in the quantum regime is independent of temperature. In the case of a universal barrier height the relaxation is exponential and we found a bulk material with this behavior. When there are identical magnetic clusters, as in polynuclear molecules, we observed jumps in both the hysteresis loops and relaxation rate, which were interpreted in terms of thermally assisted resonant tunneling between the spin levels located in the two

wells of the anisotropy. Our data on ferritin show strong departure from conventional superparamagnetic behavior. A plausible explanation for all the data is given within the model of thermally assisted resonant spin tunneling. In closing, we note that the design of new nanostructured material may lead to the discovery of new magnetic and other physical phenomena.

## References

- [1] E. M. Chudnovsky and J. Tejada, « *Macroscopic quantum tunneling of the magnetic moment* », Cambridge University Press. (1998).
- [2] E. M. Chudnovsky and L. Gunther, *Phys. Rev. Lett.* 60, 661 (1988). E. M. Chudnovsky and L. Gunther, *Phys. Rev. B* 37, 9455 (1988).
- [3] J. Tejada, X. X. Zhang, and E. M. Chudnovsky, *Phys. Rev. B* 47, 14977 (1993). J. Tejada and X. X. Zhang, *J. Magn. Magn. Mater. (invited)* 140-144, 1815 (1995).
- [4] J. Tejada, R. F. Ziolo, X. X. Zhang, *Chem. Mater. (invited review)* 8, 1784 (1996).
- [5] E. Krotenko, X. X. Zhang, and J. Tejada, *J. Magn. Magn. Mater.* 150, 119 (1995).
- [6] P.C.E. Stamp, E.M. Chudnovsky, and B. Barbara, *Int. J. Mod. Phys. B* 6, 1355 (1992).
- [7] B. Barbara and E. M. Chudnovsky, *Phys. Letters A* 145, 205 (1990).
- [8] L. Gunther and B. Barbara, « *Quantum Tunneling of Magnetization – QTM '94* ». Kluwer Academic Publishers. NATO ASI Series – Vol.301 (1995).
- [9] E. Vincent, J. Hamman, P. Preue and E. Tronc, *J. Physique*, 4, 273 (1994).
- [10] X. X. Zhang, J. M. Hernandez, J. Tejada, and R. F. Ziolo, *Phys. Rev. B* 54, 4101 (1996)
- [11] R. H. Kodama, C. L. Seaman, A. E. Berkowitz, and B. Mapple, *J. Appl. Phys.* 75, 5639 (1994).
- [12] C. Paulsen, L.C. Sampaio, B. Barbara, R. Tucoulou-Taachoneres, D. Fruchart, A. Marchand, J. L. Tholence, and M. Uehara, *Europhys. Lett.* 19, 643 (1992).
- [13] M. M. Ibrahim, S. Darwish, and M. M. Seehra, *Phys. Rev. B* 51, 2955 (1995).
- [14] Ll. Balcells, et al., *Z. Phys. B : Condens. Matter* 89, 209 (1992).
- [15] J. Tejada, X. X. Zhang, and Ll. Balcells, *Appl. Phys. (invited)* 73, 6709 (1993).
- [16] S. Gider, D. D. Awschalom, T. Douglas, S. Mann, and M. Chaparala, *Science* 268, 77 (1995). J. Tejada, *Science* 272, 424 (1996). A. Garg, *Science* 272, 424 (1996). S. Gider, D. D. Awschalom, D. P. Di Vincenzo, and D. Loss, *Science* 272, 425 (1996).
- [17] J. Tejada and X. X. Zhang, *J. Phys. : Condens. Matter.* 6, 263 (1994).
- [18] S. H. Kilcoyne and R. Cywinski, *J. Magn. Magn. Mater.* 140-144, 1466 (1995). F. Luis, *PhD. Dissertation*, University of Zaragoza (1997).
- [19] J. Tejada, X.X. Zhang, A. Roig, O. Nikolov and E. Molins, *Europhys. Letters* 30, 227 (1995).
- [20] X. X. Zhang, J. Tejada, A. Roig, O. Mikolov and E. Molins, *J. Magn. Mat.* 137, L 235 (1994).
- [21] R. Bidaux, J.E. Bouree and J. Hamman, *J. Physique* 36, 803 (1975).
- [22] J.E. Bouree and J. Hamman, *J. Physique* 36, 391 (1975).
- [23] E. M. Chudnovsky in « *Quantum Tunneling of Magnetization – QTM '94* ». L. Gunther and B. Barbara (eds.). Kluwer Academic Publishers. NATO ASI Series – Vol 301, 77 (1995).
- [24] M. A. Novak and R. Sessoli in *Quantum tunneling of Magnetization – QTM '94*, ed. by L. Gunther and B. Barbara, John Wiley & Sons, N.Y. p193 (1995).
- [25] J. R. Friedman, M. P. Sarachik, J. Tejada, and R. F. Ziolo, *Phys. Rev. Lett.* 76, 3830 (1996).
- [26] J. M. Hernandez, X. X. Zhang, F. Luis, J. Bartolome, J. Tejada, and R. F. Ziolo, *Europhys. Lett.* 35, 301 (1996). J. M. Hernandez, X. X. Zhang, F. Luis, J. Tejada, J. R. Friedman, M. P. Sarachik, and R. F. Ziolo, *Phys. Rev. B* 55, 5858 (1997).
- [27] F. Luis, J. Bartolome, J. F. Fernandez, J. Tejada, J. M. Hernandez, X. X. Zhang, and R.F. Ziolo, *Phys. Rev. B* 55, 11448 (1997).
- [28] L. Thomas, F. Lionti, R. Ballou, D. Gatteschi, R. Sessoli, and B. Barbara, *Nature* 383, 145 (1996).
- [29] J. Tejada, X. X. Zhang. E. del Barco, J. M. Hernandez, and E. M. Chudnovsky, *Phys. Rev. Lett.* 79, 1754 (1997).
- [30] J. R. Friedman, *PhD. Dissertation*, City College of New York (1997).

## About the authors

Javier Tejada is professor of Solid State Physics at the University of Barcelona. He is leading a group working on experimental magnetism which is financially supported by private industries and public agencies of Catalonia, Spain and Europe.

Tejada has published around 200 papers in scientific journals and is the inventor of 6 patents covering all the world. Very recently he has published a book entitled « *Macroscopic quantum tunneling of the magnetic moment* » edited by Cambridge University Press. The discovery of the constancy of the magnetic viscosity at low temperature and the existence of jumps in the hysteresis cycles are the experimental facts which the experimental elucidation of both magnetic tunneling and resonant spin tunneling are based upon. Professor Tejada is Doctor Honoris Causa for the City University of New York and Narcís Monturiol

medalist from the Catalan Government. Very recently he was nominated Director of the new U.B.X. laboratory for magnetic research, a joint scientific project of the University of Barcelona and Xerox Corporation.

Joan Manel Hernández is a fourth year graduate student in the group of Javier Tejada. He has been working on the magnetic properties of magnetic molecular clusters which is the topic of his PhD thesis. His main result is the complete characterization of the resonant tunneling effect discovered on Mn<sub>12</sub> molecules. During the four years in the group he has published more than 25 contributions to international publications and he owns one international patent. Actually he is focusing his work on the study of these molecular clusters at low and ultra-low temperatures.

Enrique del Barco is a third year graduate student in the group of professor Tejada. He develops his work on quantum coherence in mesoscopic magnetic systems. He has published about 10 papers in international journals and he is owner of an international patent. He actually orients his work in ultra-low temperature experiments on mesoscopic and molecular magnetic systems.

Xi Xiang Zhang is nowadays professor of the Hong Kong University of Science and Technology (HKUST). In the period 1991-1997 he worked in professor Tejada's group, during which he got his Ph.D. and published about 60 papers in international journals. He collaborated in the work that led to the discovery of quantum tunneling of the magnetic moment. He is also owner of three patents.

---